

2p/Na KLL Auger ratio could be used instead. As Figure 1 shows, this ratio varies by $\pm 12\%$, considerably more than would be expected (cf. Si 2p/Al 2p in phlogopite) if the two atoms occupied *identical* sites. However, it is known that, when Na replaces K in montmorillonite, a closely-related aluminosilicate, the smaller cation (Na^+) is displaced toward the aluminosilicate layer from the central position preferred by the larger ion (K^+) for steric reasons.¹⁴ It would thus seem entirely plausible to postulate a similar effect in muscovite. In any event, it is clear that the Na and K sites are nearly, but not totally, equivalent in this mineral. Information such as this cannot be derived from x-ray or neutron diffraction studies because of the low concentration and random distribution of the substitutional atom. Sodium comprises only about one tenth of the interlayer ions within the sampling depth (the electron inelastic mean free path is here $\sim 35 \text{ \AA}$ ¹⁵) in these specimens.

The potentialities of XPD for the study of substitutional impurities in minerals are thus clearly considerable, but the technique is not confined to geochemistry. It would, for example, seem possible to distinguish between substitutional and interstitial sites for impurity atoms present in any monocrystalline solid at low concentrations. Much further work will, however, be required to delineate fully the areas in which XPD will prove useful.

Acknowledgment. We thank the SRC for support.

References and Notes

- (1) C. Mauguin, *C. R. Hebd. Seances Acad. Sci.*, **156**, 1246 (1928).
- (2) L. Pauling, *Proc. Natl. Acad. Sci. U.S.A.*, **16**, 123 (1930).
- (3) W. L. Bragg and G. F. Claringbull, "Crystal Structures of Minerals", Bell and Sons, London, 1965.
- (4) S. W. Bailey, *Am. Min.*, **60**, 175 (1975).
- (5) K. Siegbahn, U. Gellius, H. Siegbahn, and E. Olson, *Phys. Lett. A*, **32**, 221 (1970); *Phys. Scr.*, **1**, 272 (1970).
- (6) C. S. Fadley and S. Å. L. Bergström in "Electron Spectroscopy", D. A. Shirley, Ed., North Holland, Amsterdam, 1971, p 233; *Phys. Lett. A*, **35**, 375 (1971).
- (7) S. Evans, *Proc. R. Soc. London, Ser. A*, **360**, 427 (1978).
- (8) K. Siegbahn, UUIP 940. Uppsala University Institute of Physics Preprint, 1976.
- (9) R. J. Baird, C. S. Fadley, and L. F. Wagner, *Phys. Rev. B*, **15**, 666 (1977).
- (10) R. G. Hayes, *Chem. Phys. Lett.*, **38**, 463 (1976).
- (11) J. M. Adams, S. Evans, P. I. Reid, M. J. Walters, and J. M. Thomas, *Anal. Chem.*, **49**, 2001 (1977).
- (12) This can also be seen, with hindsight, in the data of ref 5, 6, and 9, although the relative magnitude of effects due to differing site symmetries *within* specific solids has not previously been evaluated.
- (13) The Kikuchi-band treatment detailed in ref 9 implies that a marginal additional loss of structure in the O 1s diffraction pattern (relative to that for Si 2p) should result from the 26% increase in electron wavelength. (We are indebted to one of the referees for this observation.) However, we have no data for either O 1s, or the even slower F 1s, photoelectrons in which such effects are qualitatively discernible, and they may safely be neglected in the simple arguments that we advance here.
- (14) H. Pezerat and J. Méring, *C. R. Hebd. Seances Acad. Sci., Ser. D*, **285**, 529 (1967).
- (15) S. Evans, unpublished work.

John M. Adams, Stephen Evans,* John M. Thomas

Edward Davies Chemical Laboratories
University College of Wales
Aberystwyth, Dyfed, SY23 1NE, U.K.

Received December 5, 1977

Extended X-Ray Absorption Fine Structure Studies of the Hydrolytic Polymerization of Iron(III). 1. Structural Characterization of the μ -Dihydroxo-octaaquodiiron(III) Dimer¹

Sir:

The hydrolytic polymerization of iron(III) has been the subject of numerous studies² over the last several years. Aqueous solutions of iron(III) hydrolyze over a range of pH

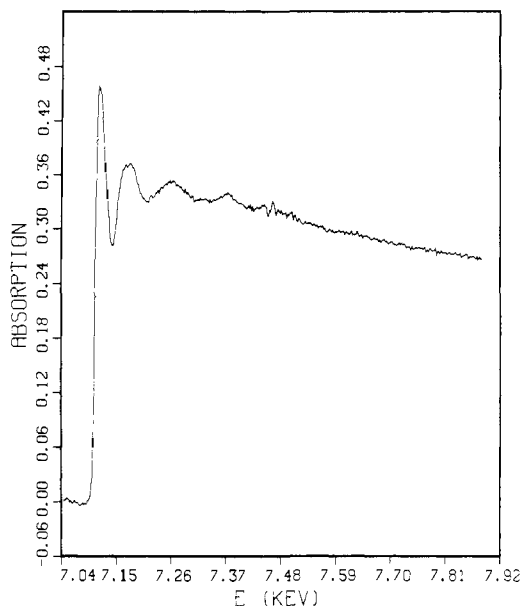


Figure 1. Raw EXAFS pattern. A plot of μx , the absorption coefficient times the effective thickness of the sample as a function of photon energy in electronvolts.

forming dimer and polymer complexes. These complexes are of interest because they display unusual magnetic properties³ and because they are believed to provide useful models⁴ for iron storage proteins. Since the complexes tend to exist only in solution, structural characterization by x-ray diffraction is usually lacking. The advent of the extended x-ray absorption fine structure (EXAFS) technique provides a unique opportunity to investigate the structures of the iron complexes in the solution phase.

The existence of the dihydroxo-bridged iron(III) dimer μ -dihydroxo-octaaquodiiron, $[(\text{H}_2\text{O})_4\text{Fe}(\text{OH})_2\text{Fe}(\text{OH})_4]^{4+}$ (1) in low pH solutions has been postulated to be the predominant specie on the basis of electrometric,⁵ thermochemical,⁶ magnetic,⁷ and spectral^{3,7} studies. No direct structural evidence has been reported to substantiate this formulation. We now wish to report structural data, based on EXAFS measurements, demonstrating the existence of the postulated dimer, 1.

The EXAFS data were taken on a modified General Electric XRD-5 diffractometer equipped with a standard line focus Mo x-ray tube, a curved germanium monochromator crystal, an automatic sample positioner, and a translatable scintillation counter. The iron solution samples were prepared by absorbing a 1.819(2) M $\text{Fe}(\text{ClO}_4)_3$ -0.023 M perchloric acid solution (pH 1.2 ± 0.2) on a piece of filter paper (12 μ thick) and sealing the paper with Parafilm to prevent evaporation and concentration changes. Figure 1 shows the resulting raw EXAFS pattern (data taken in 16 h), a plot of μx , the absorption coefficient times the effective thickness of the sample, as a function of energy in electronvolts. Following a procedure described by Lytle, Sayers, and Stern,⁸ the raw EXAFS pattern was transformed to a wave vector, $\chi(k)$, spectrum by subtracting the background and setting $k = [2m(E - E_0)/\hbar^2]^{1/2}$ where E_0 and m are, respectively, the threshold energy and mass of the ejected photoelectron (Figure 2). $\chi(k)$ may be related to interatomic distance by

$$\chi(k) = \frac{\mu(k) - \mu_0(k)}{\mu_0(k)} = 1/k \sum_i A_i f_i(k) e^{-2\sigma_i^2 k^2} \sin [2kr_i + \Phi_i(k)]$$

where $\mu_0(k)$ is a smoothly decreasing function about which $\mu(k)$ oscillates; r_i is the distance from the absorber to the i th

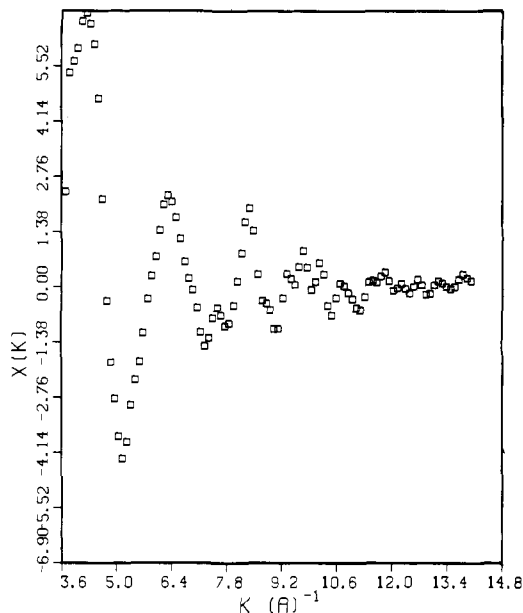


Figure 2. EXAFS pattern $\chi(k)$ after background subtraction, where k is the magnitude of the wavevector of the photoelectron.

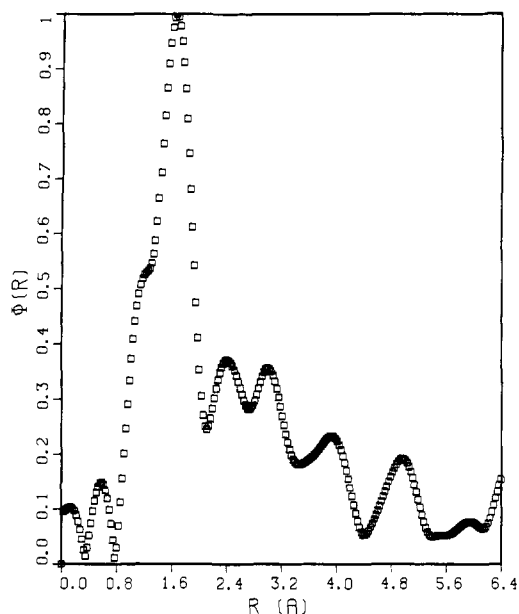


Figure 3. The Fourier transform of $k\chi(k)$ giving the function $|\phi(r)|$; no phase shifts are included in the transform.

backscatter; $A_i = N_i e^{-\gamma r_i / r_i^2}$, where N_i is number of backscatters of the i th type, and γ^{-1} is the elastic scattering length; $f_i(k)$ is the ab initio backscattering amplitude;⁹ σ_i is a Debye-Waller factor; and $\Phi_i(k)$ is an ab initio phase shift function.⁹ The function $\chi(k)$ can be Fourier transformed to give a radial distribution function $|\phi(r)|$ shown in Figure 3 in which the peak position in r space modified by a phase shift gives the distance from the absorbing atom to a backscattering shell.

The phase shifts may be obtained from similar materials with known interatomic distances but are subject to considerable uncertainty regarding chemical shifts in E_0 . In addition, the finite region in k over which $\chi(k)$ can be obtained broadens the peaks in $|\phi(r)|$ prohibiting resolution of distances that differ by less than ~ 0.4 Å. However, both of these problems can be handled for well-isolated peaks in r space by parameterizing and fitting Fourier filtered $\chi(k)$ spectra (the Fourier back-transform) of the first shell in $|\phi(r)|$.⁹ If A_i , r_i , σ_i , and E_0 are allowed to be adjustable parameters, $F(k)$ can be fit to

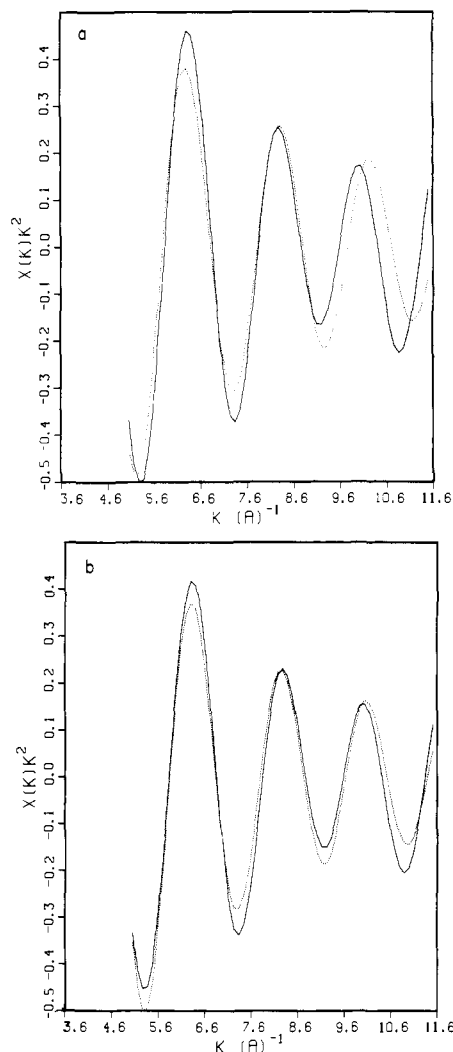


Figure 4. A nonlinear least-squares fit of the back-transform of the Fourier filtered $\phi(r)$ 1.64 Å peak between 1.07 and 2.06 Å, where the dotted line shows $k^2F(k)$ and the solid line shows $k^2\chi(k)$: (a) a single oxygen atom fit showing very poor agreement; (b) two oxygen atom fit showing the best agreement.

the k^3 weighted Fourier filtered $\chi(k)$ yielding values of r_i accurate to 0.01 Å.⁹

Following this procedure the peak at 1.64 Å (see Figure 3) in $|\phi(r)|$ was resolved into two distances at 2.03 (2) and 1.89 (4) Å. The distance at 2.03 (2) Å was assigned to a nonbridging water-iron distance, which compares favorable with Fe-OH₂ distances determined crystallographically for high spin iron(III) in $[\text{Fe}(\text{H}_2\text{O})_6][\text{NO}_3]_3 \cdot 3\text{H}_2\text{O}$ of 1.986 (7) and 2.014 (3) Å.¹⁰ Resolution of possibly different apical and equatorial bonded distances was not achieved; the 2.03 (2) Å distance is the average value. The distance of 1.89 (4) Å was attributed to a bridging hydroxyl-iron interaction, again agreeing well with an iron-bridging hydroxyl distance of 1.938 (5) Å determined in crystal studies of two "model" compounds that contain the dimeric iron unit, μ -dihydroxo-bis[2,6-pyridinedicarboxylatoaquiron(III)] and μ -dihydroxo-bis[4-hydroxo-2,6-pyridinedicarboxylatoaquiron(III)].¹¹ The relative abundances obtained for the water and hydroxyl group ligands are in a ratio of 2.5 (5):1.0, indicative of each iron(III) bound to four H₂O and two OH⁻ ligands. The quality of the fit is shown in Figure 4 where the dotted line is the fitting function $F(k)$ and the solid line is the filtered data $\chi(k)$. Figure 4a shows the poor fit which is obtained by a least-squares analysis of the data with a single oxygen at a distance of 2.00 (3) Å. Figure 4b shows the best least-squares analysis using the two

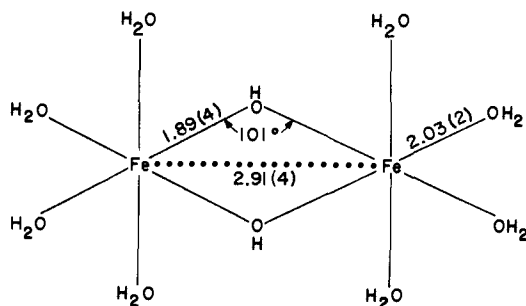
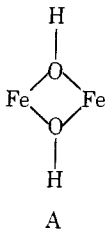


Figure 5. The proposed structure of the μ -dihydroxo-octaaquodiiron(III) dimer in a 0.023 M perchloric acid solution.

oxygen distances described above. In Figure 4 both $F(k)$ and $\chi(k)$ have been multiplied by k^2 to better illustrate the fit at high k .

The nonlinear least-squares fitting techniques were not applied to the peak in $|\phi(r)|$ at 2.42 (4) Å because of significant contributions to this peak from its neighbors.¹² However, assuming this peak is due to iron backscattering, we find an iron-iron distance of 2.91 (6) Å. We have used an empirical phase shift (linear in the k dependent term) of 0.49 (4) Å determined from an iron metal standard in making this assignment. Additional uncertainty in E_0 between standard and sample does not appreciably change the stated uncertainty in the iron-iron distance.

These results lead to the structure model for the iron(III) dimer, **1**, as that shown in Figure 5, where each iron(III) is octahedrally coordinated to two OH⁻ ligands and to four H₂O molecules. A planar ring, A, is postulated resulting in Fe-



OH-Fe bond angles of 101° and HO-Fe-OH bond angles of 79°. These angles compare well with the 103.2° Fe-OH-Fe and 76.4° HO-Fe-OH bond angles reported for the crystalline model compounds mentioned above.¹¹ The structural data for **1** is similar to the published structure of $[(\text{H}_2\text{O})_4\text{AlOH}]_2^{4+}$,¹³ where the Al-Al distance is 2.86 Å and the Al-OH-Al angle is 100.4°. The Fe-Fe distance which we have observed allows for the ionic radii increase from Al³⁺ to Fe³⁺. This iron(III) dimer model is consistent with a paramagnetic dimer with weakly coupled electron spins due to the relatively short 2.91 (6) Å Fe-Fe interaction.^{3b}

The radial distribution function $|\phi(r)|$ shows peaks above the Fe-Fe dimer distance. Rather than attributing these peaks to additional ordering of molecules about the dimer in solution, which may be a possibility, we feel that they are primarily due to high frequency noise in the data and the formation of a high molecular weight oxo- and hydroxo-bridged iron(III) polymer.^{4,12} This polymer is currently the subject of an EXAFS study in our laboratory.

We are encouraged by the present EXAFS results which show that structural data for light elements in solutions may be obtained. These results attest further to the sensitivity and subsequent value of EXAFS studies as a structural tool performed on laboratory instrumentation.

Acknowledgment. The authors wish to thank Drs. S. W. Peterson, S. Ruby, J. C. Sullivan, and J. Parks for helpful discussions and R. Telford and K. Jensen for the pH and Fe concentration measurements.

References and Notes

- (1) Work performed under the auspices of the Division of Physical Research of the U.S. Energy Research and Development Administration.
- (2) G. Spiro and P. Saltman, *Struct. Bond. (Berlin)*, **6**, 116 (1969), and references therein.
- (3) (a) L. N. Mulay and P. W. Selwood, *J. Am. Chem. Soc.*, **77**, 2693 (1955); (b) H. Schugar, C. Walling, R. B. Jones, and H. B. Gray, *ibid.*, **89**, 3712 (1967).
- (4) (a) T. G. Spiro, S. E. Allerton, J. Renner, A. Terzis, R. Bils, and P. Saltman, *J. Am. Chem. Soc.*, **88**, 2721 (1966); (b) G. W. Brady, C. R. Kurkjian, E. F. X. Lyden, M. B. Robin, P. Saltman, T. Spiro, and A. Terzis, *Biochemistry*, **7**, 2185 (1968).
- (5) B. O. A. Hedström, *Ark. Kemi*, **6**, 1 (1935).
- (6) R. M. Milburn, *J. Am. Chem. Soc.*, **79**, 537 (1955).
- (7) R. M. Milburn and W. C. Vosburgh, *J. Am. Chem. Soc.*, **77**, 1352 (1955).
- (8) F. W. Lytle, D. E. Sayers, and E. A. Stern, *Phys. Rev. B*, **11**, 4825 (1976).
- (9) (a) P. A. Lee and G. Beni, *Phys. Rev. B*, **15**, 2862 (1976); (b) P. A. Lee, B.-K. Teo, and A. L. Simons, *J. Am. Chem. Soc.*, **99**, 3856 (1977); (c) B.-K. Teo, P. A. Lee, A. L. Simons, P. Eisenberger, and B. M. Kincaid, *ibid.*, **99**, 3854 (1977).
- (10) N. J. Hair and J. K. Beattie, *Inorg. Chem.*, **16**, 245 (1977).
- (11) J. A. Thick, C. C. Ou, D. Powers, B. Vasilou, D. Mastropaolo, J. A. Potenza, and H. J. Schugar, *J. Am. Chem. Soc.*, **98**, 1425 (1976).
- (12) The peak in $|\phi(r)|$ at 3.00 (4) Å is assigned an Fe-Fe distance of 3.49 (6) Å. Because of the overlap of the 3.00 (4) Å peak and the 2.42 (4) Å peak, the nonlinear least-squares fitting routine was not applicable to the latter peak. The 3.49 (6) Å distance corresponds to the Fe-Fe distance found for the irreversibly formed iron(III) polymer. See ref 4b.
- (13) G. Johannsson, *Acta Chem. Scand.*, **16**, 403 (1962).

T. I. Morrison, A. H. Reis, Jr.*

Chemistry Division, Argonne National Laboratory
Argonne, Illinois 60439

G. S. Knapp, F. Y. Fradin, H. Chen, T. E. Klippert

Materials Science Division, Argonne National Laboratory
Argonne, Illinois 60439
Received October 12, 1977

An Electron Spin Resonance Study of the Fluxional Nature of Paramagnetic (π -Alkenyl)tris(trimethyl phosphite)iron Complexes

Sir:

We wish to report the first examples of a new class of paramagnetic compounds, $\text{Fe}[\text{P}(\text{OMe})_3]_3(\eta^3\text{-alkenyl})$, which are fluxional on the ESR time scale as revealed by characteristic ESR line-shape changes as a function of the temperature. For organic radicals there exist extensive studies of temperature-dependent line-width effects.¹ This is the first example, however, of a transition-metal organometallic radical displaying such behavior as a result of the high mobility of its ligands in a pentacoordinate structure.^{2,3}

It has been recognized for some time that the diamagnetic dimer $[(\pi\text{-allyl})\text{Fe}(\text{CO})_3]_2$ exists in equilibrium with its paramagnetic monomer.⁴ The latter can be considered as the progenitor of the organoiron radicals of this work. Addition of substituents to the allyl group as well as substitution of a carbonyl ligand with triphenylphosphine and other phosphine ligands inhibits the dimerization ostensibly for steric reasons. The tris(trimethyl phosphite) analogues of this study similarly show no tendency toward dimerization.⁵

Recently we reported the unusual 16-electron species $[\text{Fe}[\text{P}(\text{OMe})_3]_3(\eta^3\text{-cyclooctenyl})][\text{BF}_4]$ prepared by protonation of $\text{Fe}[\text{P}(\text{OMe})_3]_3(\eta^4\text{-1,3-cyclooctadiene})$.⁶ This compound undergoes a facile one-electron reduction in tetrahydrofuran (THF) with sodium amalgam to yield an isolable, air-sensitive, but thermally quite stable, dark blue-green paramagnetic species **1**, shown in a possible pseudo-square-pyramidal structure. Dilute solutions of this compound in hydrocarbon solvents are emerald green and afford ESR